CORRELATION BETWEEN THE ELECTRONIC STRUCTURE OF QUINAZOLINE DERIVATIVES AND THE ACTIVITY OF THE NTR1 RECEPTOR

CARLOS SOLOAGA ARDILES, CRISTIAN CASTRO RODRIGUEZ AND JULIO SURCO LUQUE*

Departamento de Química, Universidad de Tarapacá, Av. General Velásquez 1775, P.O. Box 7-D Arica, Chile.

ABSTRACT

The relationship between ectopic neurotensin expression (NTS) and tumor carcinoma invasion has produced studies that point to allosteric modulation of the regular NTR1 receptor. The use of quinazoline-derived drugs has shown excellent results in the regulation of the biological process mentioned. This study aims to establish the relationship between the electronic structure of quinazoline derivatives and the biological activity (expressed as EC50) that process in the NTR1 receptor, to propose a 2D pharmacophore. For this purpose, the Klopman-Peradejordi-Gómez (KPG) methodology was used. Calculations are included within the functional density theory (DFT) using the B3LYP / 631G theory level (d, p). The results concerning the biological activity are mainly driven by the interactions at the orbital-orbital level and by charges. These results can be used to propose new quinazoline derivatives with a better response in allosteric modulation of the NTR1 receptor.

Keywords: NTR1 receptor, quinazoline derivatives, KPG method (QSAR).

INTRODUCTION

Neurotensin (NT), a tridecapeptide of the brain-intestine, has a dual role as a neurotransmitter or neuromodulator in the central nervous system (CNS) [1]. The actions of NT and related signal transduction depend on the recognition of the peptide in the plasma membrane of the cells by three specific receptors, called NTR1, NTR2, and NTR3 [2]. For non-neuronal systems, the main roles of neurotensin in the gastrointestinal and cardiovascular system have been demonstrated [3]. Neurotensin is located in the intestinal mucosa (endocrine N cells), where it is believed to be involved in intestinal contraction [4,5]. The effects of NTS are mediated by three subtypes of neurotensin receptors (NTR), those already mentioned; NTR1, NTR2, and SORT1 [6]. Among these receptors, NTR1 mediates most of the biological functions of NTS. This is a receptor coupled to the G protein that is widely expressed throughout the central nervous system, where it acts as a neuromodulator [7, 8]. Some studies show a significant relationship between ectopic expression of NTS and tumor invasion in hepatocellular carcinoma (HCC). In primary CHC tissues, the co-expression of NTS and neurotensin receptor 1 is a poor prognostic factor related to aggressive biological behaviors and poor clinical prognosis [8, 9]. Of the three subtypes of neurotensin receptors (NTR), the NTR1 receptor is the most widely studied. This receptor mediates most of the known neurotensin effects, which makes it an interesting therapeutic objective. Despite the therapeutic promise of NTR1, the development of ligands for this receptor has been hindered [10]. Results have been reported, in which the authors propose a series of quinazoline-derived compounds, which showed a good response in allosteric modulation in the NTR1 receptor [4].

The present work aims to relate the electronic structure of quinazoline derivatives and biological activity (expressed as EC50) in the NTR1 receptor, to improve ligands that favor allosteric modulation in this receptor. The KPG (Klopman-Peradejordi-Gómez) method will be used, which employs local reactivity indices, based on quantum chemistry calculations and multiple linear regression statistics (LMRA) [11]. This method has been widely used when seeking to propose a 2D pharmacophore, which specifies not only the atoms involved but also the nature of the type of binding between the ligand and the receptor [12-14].

METHODS, MODELS, AND CALCULATIONS

The KPG method has been previously reported in several articles. In order not to extend in its explanation, the reader is left with some bibliographical references for further study [14-17]. This method is based on the following general equation:

$$\log(BA) = a + bM_{D_i} + c\log[\sigma_{D_i}/(ABC)^{1/2}] + \sum_j[e_jQ_j + f_jS_j^E + s_jS_j^N] + \sum_j\sum_m[h_j(m)F_j(m) + x_j(m)S_j^E(m)] \quad (1)$$

$$+ + \sum_j\sum_m[r_j(m')F_j(m') + t_j(m')S_j^N(m')] + \sum_j[g_j\mu_j + k_j\eta_j + o_j\omega_j + z_j\varsigma_j + w_jQ_j^{max}]$$

where $a, b, c, e_j, f_j, s_j, h_j(m), x_j(m), r_j(m), t_j(m), g_j, k_j, o_j, z_j, w_j$, are constants to determine. M_{D_i} Is the mass of the molecule (drug), σ_{D_i} is the el number of

symmetry, ABC: product of the moments of inertia of the ligand on the three main axes of rotation, ABC: product of the moments of inertia of the ligand on the three main axes of rotation, Q_j: net charge of the atom j, S_j^E the total atomic electrophilic superdelocalizabilities of atom j, S_j^N: is the total atomic nucleophilic superdelocalizabilities of atom j, $F_j(m)$ ($F_j(m')$): is the electron population (Fukui index) of the occupied (vacant) MO m (m') localized on atom j, $S_j^E(m)$ is the atomic electrophilic superdelocalizability of MO m localized on atom j, $S_j^N(m')$: is the atomic nucleophilic superdelocalizability of MO m´ localized on atom j, μ_j: is the local atomic electronic chemical potential of atom j, η_j: Is the local atomic hardness of atom j, ω_j: Is the local atomic electrophilicity of atom j ς_j: Is the local atomic softness of atom j, Q_j^{max}: is the maximum amount of electronic charge that atom j that atom j may accept from another site, O_k: is the orientational parameters of the k_{th} substituent k.

Electronic populations are considered when assigning a localized molecular orbital to a specific atom. In this method, to assign a local OM to an atom, the latter must present electronic populations equal to or higher than 0.01, according to Mulliken population analysis [14, 18]. In this form, it is possible to find the local HOMO of atom i (that is, the highest occupied MO that has an electron population of 0.01 electron or more in atom i) and the local LUMO (usually denoted by HOMOi * and LUMOi * respectively).

SELECTION OF MOLECULES

The selected molecules and their biological activities (Table [a]) were reported in a previous study [4]. The molecules under study have a common structure, where the substituents vary (Figure 1). The experimental results obtained in the reference study (biological activity) were obtained *in vivo*, and are expressed as a mean effective concentration (EC50). The EC50 indicates the concentrations in µM of the compound, which generate 50% of the allosteric modulation in the NTR1 receptor.
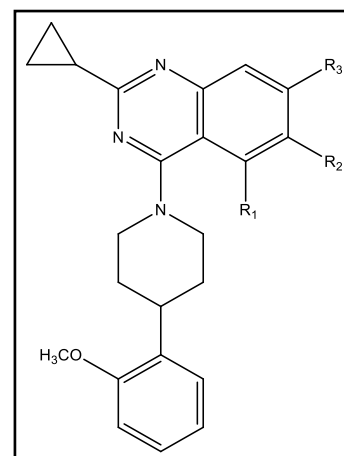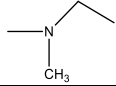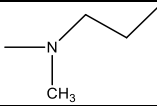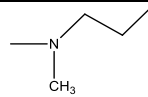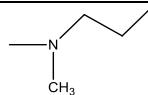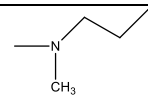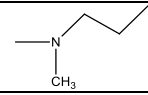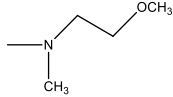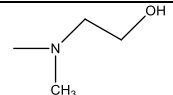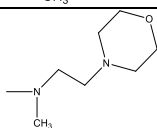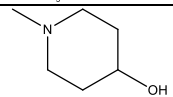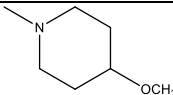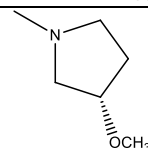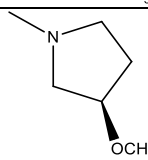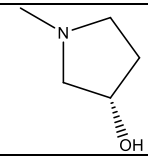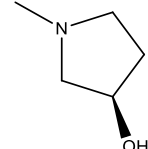

Figure 1. Common Structure.

Corresponding author email: delgaradh@gmail.com

Table [a]. Selected molecules and their activities (EC50)

Molecule	Log EC50	R_1	R_2	R_3
1	0.02	H	-OCH_3	OCH_3
2	-0.05	H	-$N(CH_3)_2$	H
3	-0.25	H		H
4	0.83		H	H
5	-0.14	H		H
6	1.00	H	H	
7	-0.01	H		CH_3
8	0.48	H		F
9	0.05	H		H
10	-0.32	H		H
11	-0.09	H		H
12	0.83	H		H
13	0.44	H		H
14	-0.09	H		H
15	-0.19	H		H
16	0.01	H		H
17	-0.36	-H		-H

CALCULATIONS

The electronic structure of each molecule was obtained through the theory of functional density (DFT) at the level of theory B3LYP/6-31G (d, p), using Gaussian 09 software. Local reactivity indices were calculated using the D-CENT-QSAR software [19].

For the group of molecules under study, the hypothesis of a typical skeleton was formulated (Figure 2). This hypothesis contains a set of atoms common to each of the molecules under study. Each atom of the common skeleton will be determined different indices of local reactivity, which will be related, through multiple regression analysis, with the logarithms of the biological activities. These results will allow obtaining the atoms that participate in the interaction with the receptor and the type of interaction involved. The variation of the values of a set of local reactivity indices, of one or more atoms belonging to the common skeleton, indicates the variation of the allosteric modulation in the NTR1 receptor [14, 19].

Figure 2. Common skeleton Numeration.

RESULTS

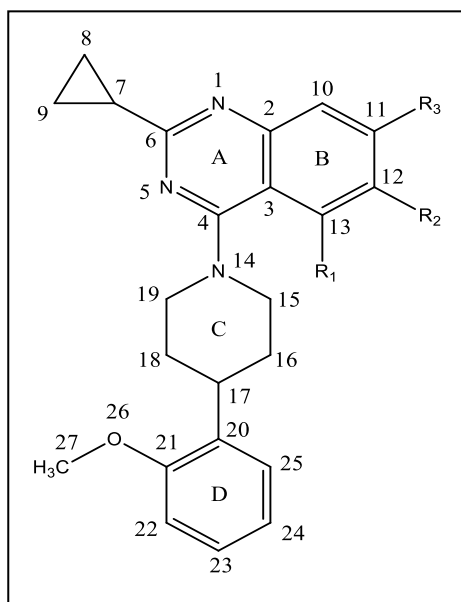It is noteworthy to highlight that the reactivity indexes on the employed method are not normalized, given that they have a concrete physical meaning. This concrete physical meaning is particularly important to sustain the physical meaning of the equation and the comparison with studies in which different molecules are used in the interaction with the same receptor.

Table [c]. Squared correlation coefficients for the variables appearing in Eq. 9.

The method employed does not need external validation due to its formal mathematical structure [14].

Results for the activity at NTR1 receptor

The best statistically significant equation obtained for the set I, is the following:

$$LOG(EC50) = 16.80 - 42.49 S_4^E(HOMO-2)^* - 48.17 F_{14}(HOMO-1)^* + 52.66 S_3^E \quad (9)$$
$$+ 4.79\mu_{21} + 4.82 S_{11}^E(HOMO-2)^* - 38.58 Q_{19} - 6.67 F_{11}(LUMO+2)^*$$
$$+ 10.91 S_1^N(LUMO+1)^*$$

with n=17, R= 0.98, R²= 0.95, adj. R²= 0.91, F (8, 8) = 21.21 (p < 0.0001) and a standard error of estimate of 0.12. No outliers were detected, and no residuals fall outside the ±2σ limits.

In equation 9 $S_4^E(HOMO-2)^*$ it is the Fukui index of the second-highest occupied local molecular orbital in atom 4, $F_{14}(HOMO-1)^*$ is the Fukui index of the second-highest occupied local molecular orbital in atom 14, S_3^E is the total electrophilic superdelocalizability in atom 3, μ_{21} is the local electronic chemical potential in atom 21, $S_{11}^E(HOMO-2)^*$ is the electrophilic superdelocalizability of the third-highest occupied local molecular in atom 11, Q_{19} is the net-charge located in atom 19, $F_{11}(LUMO+2)^*$ is the Fukui index of the third lowest empty local molecular orbital in Atom 11, $S_1^N(LUMO+1)^*$ is the nucleophilic superdelocalizability of the second-lowest empty local molecular orbital in atom 1.

Table [b]: Beta coefficients and t-test for significance of the coefficients in Eq. 9.

	Beta	**t (8)**	**p-level**
$S_4^E(HOMO-2)^*$	-1.84	-9.16	> 0.00001
$F_{14}(HOMO-1)^*$	-1.89	-7.65	> 0.00006
S_3^E	0.98	6.65	> 0.0001
μ_{21}	0.67	5.03	> 0.001
$S_{11}^E(HOMO-2)^*$	0.49	4.33	> 0.002
Q_{19}	-1.05	-5.20	> 0.0008
$F_{11}(LUMO+2)^*$	-0.48	-3.41	> 0.001
$S_1^N(LUMO+1)^*$	0.50	3.05	> 0.02

Squared correlation coefficients for the variables appearing in Eq.9.

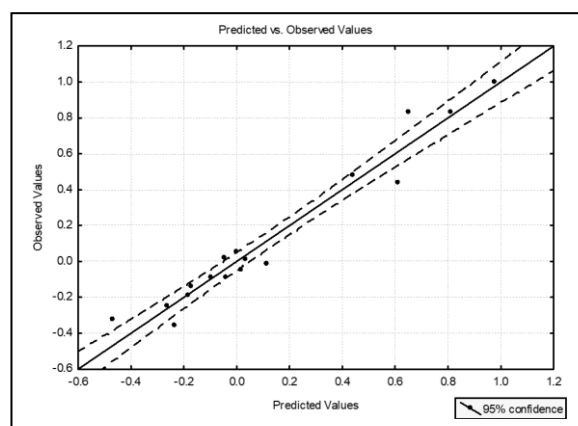|	$S_4^E(HOMO-2)^*$	$F_{14}(HOMO-1)^*$	S_3^E	μ_{21}	$S_{11}^E(HOMO-2)^*$	Q_{19}	$F_{11}(LUMO+2)^*$
$F_{14}(HOMO-1)^*$	0.21	1.00					
S_3^E	0.08	0.06	1.00				
μ_{21}	0.00	0.01	0.03	1.00			
$S_{11}^E(HOMO-2)^*$	0.08	0.28	0.05	0.22	1.00		
Q_{19}	0.10	0.35	0.06	0.04	0.06	1.00	
$F_{11}(LUMO+2)^*$	0.29	0.01	0.05	0.12	0.11	0.23	1.00
$S_1^N(LUMO+1)^*$	0.36	0.00	0.04	0.14	0.00	0.07	0.24

Figure 3. Plot of predicted vs. observed EC50 values (Eq. 9).

Table 3 shows the beta coefficients and the results of the t-test for the importance of coefficients in the equation. Table [c] shows low internal correlations between independent variables (the highest obtained value was 0.36). Figure 3 shows the graph of observed values versus calculated EC50 log values. Statistical data referring to the equation shows that equation 9 is statistically significant and represents the variation of 8 reactivity indices that belong to the common skeleton and accounts for approximately 91% of the variation in biological activity.

To propose the type of interaction for each atom of equation 9, the three highest local occupied molecular orbitals (HOMO)* and the three lowest local empty voids (LUMO)*. These molecular orbitals are shown in the following table.

Table [d]. Nomenclature: Molecule Set I (HOMO) / (HOMO-2) * (HOMO-1) * (HOMO) * - (LUMO) * (LUMO + 1) * (LUMO + 2) *.

Mol.	Atom 1	Atom 3	Atom 4	Atom 11
1(112)	109σ110σ112π-113π114π117π	109σ110π112π-113π114π117π	109σ110π112π-113π114π117π	108π110π112π-113π114π117π
2 (108)	105σ106σ108π-109π110π113π	105σ106π108π-109π110π113π	105σ106π108π-109π110π113π	104π106σ108π-109π110π113π
3 (112)	109σ110π112π-113π114π117π	109σ110π112π-113π114π117π	109σ110π112π-113π114π117π	108σ110π112π-113π114π117π
4 (116)	113σ115π116σ-117π118σ121σ	112π113σ115π-117π118π121π	113σ115π116σ-117π118π121π	112π115π116π-117π118π121π
5 (108)	105σ106σ108π-109π110π113π	105σ106π108π-109π110π113π	105σ106π108π-109π110π113π	104π106π108π-109π110π113π
6 (116)	113σ115σ116σ-117π118π121π	113σ115π116π-117π118π121π	112π113σ115π-117π118π121π	109π110π116π-117π118π121π
7 (120)	118σ119π120π-121π122π125π	117σ118π120π-121π122π125π	117σ118π120π-121π122π125π	116σ118π120π-121π122π125π
8 (120)	117σ118π120π-121π122π125π	117σ118π120π-121π122π125π	117σ118π120π-121π125π126π	116σ118π120π-121π122π125π
9 (120)	118π119π120π-121π122π125π	117σ118π120π-121π122π125π	117σ118π120π-121π122π125π	116σ118π120π-121π122π125π
10 (116)	113σ114π116π-117π118π121π	113σ114π116π-117π118π121π	113σ114π116π-117π118π121π	112π114π116σ-117π118π121π
11 (135)	132σ134π135π-136π137π140π	132π134π135π-136π137π140π	132π134π135π-136π137π140π	130π132π135π-136π137π140π
12 (123)	120σ121σ123π-124π125π128π	120σ121π123π-124π125π126π	120σ121π123π-124π125π128π	119π121π123π-124π125π126π
13 (127)	125σ126π127π-128π129π132π	124σ125π127π-128π129π130π	124σ125π127π-128π129π132π	123π125π127π-128π129π130π
14 (123)	121π122π123π-124π125π128π	120π121π123π-124π125π128π	120π121π123π-124π125π128π	119π121π123π-124π125π128π
15 (123)	120σ121π123π-124π125π128π	120σ121π123π-124π125π126π	120σ121π123π-124π125π128π	119π121π123π-124π125π126π
16 (119)	116σ117σ119π-120π121π124π	116σ117π119π-120π121π124π	116σ117π119π-120π121π124π	115π117π119π-120π121π124π
17 (119)	116σ117π119π-120π121π124π	116σ117π119π-120π121π124π	116σ117π119π-120π121π124π	115π117π119π-120π121π124π

Mol.	Atom 14	Atom 19	Atom 21
1(112)	109π110π112σ-113σ117π119σ	109σ110σ112σ-113σ117σ119σ	102σ107π111π-115π116π118π
2 (108)	105σ106π108σ-109π113σ115π	103σ104σ106σ-109σ115σ121	98σ104π107π-111π112π114--
3 (112)	110σ111π112σ-113π117π120π	102σ108π110σ-113σ120σ124σ	108π110σ111π-115π116π119π
4 (116)	113π115π116π-117σ121σ122σ	112σ115π116σ-117σ121σ123σ	106σ111π114σ-119π120π124π
5 (108)	106π107π108σ-109π113π117π	104σ106σ107σ-109σ111π116σ	104σ106σ107π-111π112π115π
6 (116)	112π113π115π-117π121π125π	106π112σ115σ-117σ119σ121σ	106σ111π114π-119π120π123π
7 (120)	118σ119π120σ-121π125π127π	116σ118σ119σ-121σ123σ125σ	115π118π119π-123π124π127π
10 (116)	114σ115π116σ-117π121π125π	112σ114σ115σ-117σ119σ121σ	112π114π115π-119π120π124π
10 (116)	114σ115π116σ-117π121π125π	112σ114σ115σ-117σ119σ121σ	112π114π115π-119π120π124π
10 (116)	114σ115π116σ-117π121π125π	112σ114σ115σ-117σ119σ121σ	112π114π115π-119π120π124π
11 (135)	133π134π135σ-136π140π146π	130σ132σ133π-136σ138σ140σ	130π132π133π-138π139π142π
12 (123)	121σ122π123σ-124π128π133π	112σ119σ121σ-124σ132σ135σ	119π121σ122π-126π127π131π
13 (127)	125σ126π127σ-128σ132π137π	123σ125σ126π-128σ136σ141σ	123π125π126π-130π131π134π
14 (123)	121σ122π123σ-124π128π133π	119σ121σ122σ-124σ126σ128σ	119π121π122π-126π127π131π
15 (123)	121σ122π123σ-124π128π133π	112σ119σ121σ-124σ128σ132	119π121π122π-126π127π131π
16 (119)	116σ117σ119σ-120π124π127π	108σ115σ117σ-120σ124σ127σ	108π114π118π-122π123π128π
17 (119)	117π118π119σ-120π124π127π	115σ117σ118σ-120σ122σ124σ	115π117π118π-122π123π126π

DISCUSSION

The beta values represented in Table 2 show that the order of importance of the variables follows the subsequent order:

$$F_{14}(HOMO-1)^* > S_4^E(HOMO-2)^* > Q_{19} > S_3^E > \mu_{21} > S_1^N(LUMO+1)^* >$$

$$S_{11}^E(HOMO-2)^* \approx F_{11}(LUMO+2)^*$$

The process is governed by weak interactions that depend on the electronic populations and the energy of the OMs for N1, C3, C4, C11, C14, C21, while for C19 (Figure 2), it depends on the net charge on this atom.

The variable $S_1^N(LUMO+1)^*$ will not be discussed due to the high value of p (Table [b]).

The discussion of the results will be conveyed knowing that: Fukui indices are always positive, total and partial electrophilic superdelocalizabilities are negative, the charge of atom 19 is positive, and the electronic chemical potential is always negative.

Atom 14 is a nitrogen of ring C (Figure 2). High values of $F_{14}(HOMO-1)^*$ are associated with high biological activity. According to Table [d], its OMs are of σ o π nature. Most of the local OM molecules coincides with molecular HOMO, which indicates a high reactivity of the local OM. It is suggested that atom 14 is interacting with a deficient center in electrons through its first two busiest local molecular orbitals [20, 21].

Atom 4 is a carbon of aromatic ring A (Figure 2). Lower negative values of $S_4^E(HOMO-2)^*$ can be associated with high biological activity. This carbon is attached to two nitrogen atoms, N5 (ring A) and N14 (ring C). The OM $(HOMO)^*$, $(HOMO-1)^*$, $(HOMO-2)^*$, are of π nature, where local HOMO coincides with the molecular HOMO (Table [d]). The high electronegativity of nitrogen would decrease the electron density in the carbon atom 4. It is suggested that atom 4 interacts with a rich center in electrons [22, 23].

Atom 3 is a carbon that links rings A and B (Figure 2). High negative values of S_3^E are related to a high activity of receptor NTR1. Table [d] shows local OMs of this carbon are of π nature. It is suggested that this atom interacts with an electron-deficient π center [22].

Atom 21 is an atom of carbon attached to O26 (metoxi group) (Figure 2). A high affinity of the receptor is associated with negative values for μ_{21}. This index is the middle point between energies (HOMO) * and (LUMO) *. Table [d] shows that all local MO have a π nature, (LUMO) * is energetically far from molecular LUMO and (HOMO) * is very close to molecular HOMO. Therefore, to obtain more negative values for μ, a substituent can be attached to the atom 21 such that LUMO o LUMO + 1 of molecule localized in this atom, making empty MO more reactive, improving its capacity to take electrons. It is suggested that atom 21 is probably interacting with a site (atom or residue) with a busy OM σ (sometimes called the apolar region) [14, 23].

Atom 19 is a carbon of the saturated ring C (Figure 2). Negative values of Q_{19} associated to a high biological activity. Its local OMs are of σ nature (Table [d]). This carbon is attached to a nitrogen atom, which would mean that the high electronegativity of the latter would decrease the electronic density of carbon 19. It is suggested that this atom interacts by electrostatic bonding with a negatively charged center [24-26].

A particular situation results in the analysis of the results for atom 11. This atom, is a carbon of the aromatic ring B (Figure 2). According to Table [d], its local OMs are of π nature. The fact that they relate to the high activity of NTR1 high values of $S_{11}^E(HOMO-2)^*$ and $F_{11}(LUMO+2)^*$ implies that this carbon interacts with a deficient center of electrons in the first case and a rich electrons center in the second case, at the same time [27, 28]. It is suggested that for $S_{11}^E(HOMO-2)^*$ the interaction occurs with empty OM from a receptor site; meanwhile, for $F_{11}(LUMO+2)^*$ the interaction occurs with a busy OM. $(HOMO-2)^*$ and $(LUMO+2)^*$ are of π nature in atom 11, where local HOMO and LUMO coincide with molecular HOMO and LUMO. This suggests that, in the case of $F_{11}(LUMO+2)^*$ a busy OM overlap of the receptor would occur which increases the electronic density over carbon, while in $S_{11}^E(HOMO-2)^*$ could generate an interaction by giving electronic density to a receptor site by interaction π-π or σ-π, which will allow stabilizing the electronic density on itself.

Both facts are compatibles. Another possible interpretation of this situation is a significant difference in the beta values or a high correlation between both variables. Nevertheless, this situation does not occur, as can be seen in Table 3 and in Table 4 [29, 30].
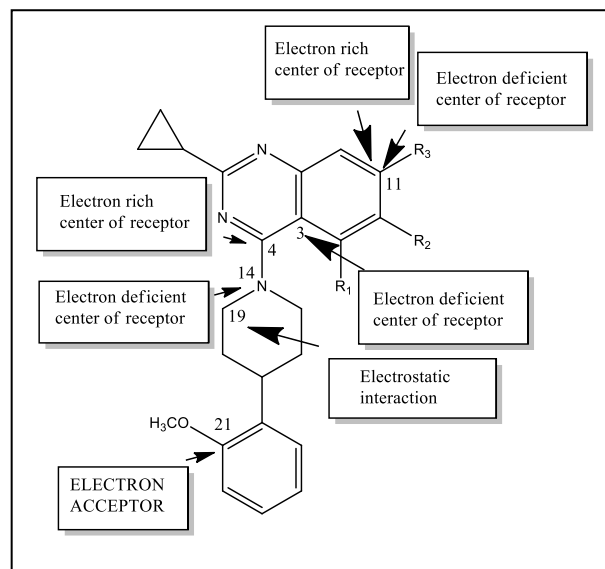
These results are represented in Figure 4.

Figure 4. 2D pharmacophore for receptor binding NTR1.

CONCLUSIONS

Through the use of LMRA, a statistically significant equation was obtained for the variation of the biological activity generated by quinazoline derivatives, concerning the variation of a set of local atomic reactivity indices. From the results, a 2D pharmacophore was proposed, in which it is shown that the biological process is governed mainly by weak interactions at the orbital-orbital level and by loads. These results may facilitate the synthesis of quinazoline-derived drugs, with high allosteric modulation (antagonist) in the NTR1 receptor.

REFERENCES

1. Kato HE, Zhang Y, Hu H, Suomivuori C-M, Kadji FMN, Aoki J, et al. Conformational transitions of a neurotensin receptor 1–G i1 complex. Nature 2019:1.
2. Hwang JR, Baek MW, Sim J, Choi H-S, Han JM, Kim YL, et al. Intermolecular cross-talk between NTR1 and NTR2 neurotensin receptor promotes intracellular sequestration and functional inhibition of NTR1 receptors. Biochem Bioph Res Co 2010;391:1007-13.
3. Choi S-Y, Chae H-D, Park T-J, Ha H, Kim K-T. Characterization of high affinity neurotensin receptor NTR1 in HL-60 cells and its down regulation during granulocytic differentiation. Brit J Pharmacol 1999;126:1050.
4. Pinkerton AB, Peddibhotla S, Yamamoto F, Slosky L, Bai Y, Maloney PR, et al. Discovery of b-Arrestin Biased, Orally Bioavailable and CNS Penetrant Neurotensin Receptor 1 (NTR1) Allosteric Modulators. J Med Chem 2019.
5. Onaga T, Shimoda T, Ohishi T, Yasui Y, Hayashi H. Role of neurotensin in the regulation of gastric motility in healthy conscious sheep. Small Ruminant Res 2019;172:31-41.
6. Labbé-Jullié C, Barroso S, Nicolas-Etève D, Reversat J-L, Botto J-M, Mazella J, et al. Mutagenesis and modeling of the neurotensin receptor NTR1 identification of residues that are critical for binding SR 48692, a nonpeptide neurotensin antagonist. J Med Chem 1998;273:16351-7.
7. Pelaprat D. Interactions between neurotensin receptors and G proteins. Peptides 2006; 27:2476-87.

8. Ye Y, Long X, Zhang L, Chen J, Liu P, Li H, et al. NTS/NTR1 co-expression enhances epithelial-to-mesenchymal transition and promotes tumor metastasis by activating the Wnt/β-catenin signaling pathway in hepatocellular carcinoma. Oncotarget 2016;7:70303.

9. Gahbauer S, Pluhackova K, Böckmann RA. Closely related, yet unique: Distinct homo-and heterodimerization patterns of G protein coupled chemokine receptors and their fine-tuning by cholesterol. Plos Comput Biol 2018;14:e1006062.

10. Griebel G, Holsboer F. Neuropeptide receptor ligands as drugs for psychiatric diseases: the end of the beginning? Nat Rev Drug Discov 2012;11:462.

11. Gómez-Jeria JS. 45 Years of the KPG Method: A Tribute to Federico Peradejordi. Journal of Computational Methods in Molecular Design 2017;7:17-37.

12. Muñoz-Gacitúa D, Gómez-Jeria JS. Quantum-chemical study of the relationships between electronic structure and anti-influenza activity. 2. The inhibition by 1H-1, 2, 3-triazole-4-carboxamide derivatives of the cytopathic effects produced by the influenza A/WSN/33 (H1N1) and A/HK/8/68 (H3N2) strains in MDCK cells. Journal of Computational Methods in Molecular Design 2014;4:48-63.

13. Gómez-Jeria JS. A quantum chemical analysis of the relationships between electronic structure, PAK1 inhibition and MEK phosphorylation in a series of 2-arylamino-4-aryl-pyrimidines. SOP Trans Phys Chem 2014;1:10-28.

14. Kpotin GA, Bédé AL, Houngue-Kpota A, Anatovi W, Kuevi UA, Atohoun GS, et al. Relationship between electronic structures and antiplasmodial activities of xanthone derivatives: a 2D-QSAR approach. Stuc Chem 2019:1-10.

15. Gómez-Jeria JS. A new set of local reactivity indices within the Hartree-Fock-Roothaan and density functional theory frameworks. Can Chem Trans 2013;1:25-55.

16. Gómez-Jeria J. Calculation of the nucleophilic superdelocalizability by the CNDO/2 method. J Pharm Sci 1982;71:1423.

17. Gómez-Jeria JS. Modeling the drug-receptor interaction in quantum pharmacology. Molecules in Physics, Chemistry, and Biology: Springer; 1989; 215-31.

18. Gautier, Kankinou & Kpotin, Gaston & Mensah, Jean-Baptiste & Gómez-Jeria, Juan-Sebastián.. Quantum-Chemical Study of the Relationships between Electronic Structure and the Affinity of Benzisothiazolylpiperazine Derivatives for the Dopamine Hd2l and Hd3 Receptors. Pharm. Chem. J. 2019; 6: 73-90.

19. Gómez-Jeria JS. An empirical way to correct some drawbacks of mulliken population analysis. J. Chil. Chem. Soc 2009;54:482-5.

20. Kpotin GA, Gómez-Jeria JS. A Quantum-chemical Study of the Relationships Between Electronic Structure and Anti-proliferative Activity of Quinoxaline Derivatives on the HeLa Cell Line. Chemistry 2017;5:59-68.

21. Soro D, Ekou L, Ouattara B, Kone MG-R, Ekou T, Ziao N. DFT Study, Linear and Nonlinear Multiple Regression in the Prediction of HDAC7 Inhibitory Activities on a Series of Hydroxamic Acids. Comput Mol Biosci 2019;9:63.

22. Valdebenito-Gamboa J, Gómez-Jeria JS. A theoretical analysis of the relationships between electronic structure and HIV-1 integrase inhibition and antiviral activity of a series of naphthyridinone derivatives. Der Pharma Chem 2015;7:543-55.

23. Gómez-Jeria JS, Cornejo-Martínez R. A DFT study of the inhibition of human phosphodiesterases PDE3A and PDE3B by a group of 2-(4-(1H-tetrazol-5-yl)-1H-pyrazol-1-yl)-4-(4-phenyl) thiazole derivatives. Der Pharma Chem 2016;8:329-37.

24. Soloaga Ardiles C, Cárcamo Vega J. Theoretical analysis of the relationship between the electronic structure and its inhibitory action in the p2x7r receptor of a series of 2-hydroxy-1, 4-naphthoquinones derivatives. J. Chil. Chem. Soc 2018;63:4205-10.

25. Gómez-Jeria JS, Valdebenito-Gamboa J. A quantum-chemical analysis of the antiproliferative activity of N-3-benzimidazolephenylbisamide derivatives against MGC803, HT29, MKN45 and SW620 cancer cell lines. Der Pharma Chem 2015;7:103-21.

26. Kpotin G, Atohoun SY, Kuevi A, Kpota-Hounguè A, Mensah J-B, Jeria JG. A Quantum-Chemical study of the Relationships between Electronic Structure and Trypanocidal Activity against Trypanosoma Brucei Brucei of a series of Thiosemicarbazone derivatives. Pharm Lett 2016;8:215-22.

27. Gómez Jeria J, Kpotin GA. Some remarks on the interpretation of the local atomic reactivity indices within the Klopman Peradejordi Gomez (KPG) method. I. Theoretical analysis. 2018.

28. Anatovi W, Kpotin GA, Kuevi UA, Houngue-Kpota A, Atohoun GS, Mensah J-B, et al. A DFT study or the relationship between the electronic structure and the antiplasmodial activity of a series of 4-anilino-2-trichloromethylquinazolines derivatives. World Sci News 2017;88:138-51.

29. Gómez-Jeria J, Valdebenito-Gamboa J. A DFT Study of the Relationships between the Electronic Structures of a series of 2, 4, 5-Trisubstituted Pyrimidines and their Inhibition of four Cyclin-dependent Kinases and their Anti-Proliferative Action against HCT-116 and MCF-7 Cell Lines. Der Pharma Chem 2014;6:383-406.

30. Gómez-Jeria JS, Abarca-Martínez S. A theoretical approach to the cytotoxicity of a series of β-carbolinedithiocarbamate derivatives against prostatic cancer (DU-145), breast cancer (MCF-7), human lung adenocarcinoma (A549) and cervical cancer (HeLa) cell lines. Der Pharma Chem 2016;8:507-26.